Eur. Phys. J. B **10**, 623–633 (1999)

THE EUROPEAN PHYSICAL JOURNAL B

EDP Sciences

Low frequency elastic properties of neutron-irradiated quartz. Comparison with glasses*

J. Classen[1,a], I. Rohr[1], C. Enss[1], S. Hunklinger[1], and C. Laermans[2]

[1] Institut für Angewandte Physik, Universität Heidelberg, Albert-Ueberle-Strasse 3–5, 69120 Heidelberg, Germany
[2] Department of Physics, Katholieke Universiteit Leuven, Celestijnenlaan 200D, 3001 Leuven, Belgium

Received 23 October 1998

Abstract. Neutron-irradiated quartz is a promising model system to learn more about the low-energy excitations (tunneling states) in vitreous silica and in similar glasses. We present the first systematic study of the elastic properties of neutron-irradiated quartz at low frequencies and very low temperatures. Using the vibrating reed technique at frequencies of several kHz we have measured the sound velocity and internal friction of six quartz crystals irradiated with different neutron doses over a wide range of temperatures (7 mK–300 K). The results are analyzed using the tunneling model and several extensions of this theory. Comparisons are made with recent low-frequency measurements on normal and compacted vitreous silica and with ultrasound experiments on neutron-irradiated quartz.

PACS. 62.65.+k Acoustical properties of solids – 61.80.Hg Neutron radiation effects

1 Introduction

When crystals are bombarded by high energy neutrons their regular structure may be severely damaged by collisions between the neutrons and the atomic nuclei. The type and degree of radiation-induced disorder depends on the crystal structure and on the strength of the atomic bonds as well as on the number and energy of the incident neutrons. Radiation damage has been studied particularly intensively for α-quartz. Among other reasons this interest results from the idea that neutron-irradiated quartz might be a promising model system to learn more about the tunneling states in vitreous silica. These localized low-energy excitations [1] are found in virtually all amorphous solids in similar number but their microscopic origin is still a matter of debate. Since the disorder in irradiated quartz can be gradually enhanced by an increase of the neutron dose these crystals offer the opportunity to study systematic relations between the radiation-induced damage and the number density, the dynamics, and perhaps the nature of tunneling states.

It is known from X-ray scattering experiments that the collisions between neutrons and atomic nuclei in quartz lead to the formation of amorphous clusters of radius ~ 10 Å embedded in a slightly distorted but still crystalline matrix [2–4]. With increasing neutron dose the number (and to a smaller extent the size [4]) of these amorphous regions increases, and for neutron doses above $\sim 1 \times 10^{20}$ n/cm^2 a completely amorphous phase — the so-called metamict phase — develops with a density about 14% smaller than in unirradiated quartz but still almost 3% higher than in vitreous silica.

Over the past years the high frequency elastic properties of neutron-irradiated quartz have been intensively studied above 0.3 K by means of ultrasonic experiments [5–11]. Some particularly interesting results of these measurements were:

i) The number of tunneling states increases approximately linearly with increasing neutron dose for small doses; it saturates for doses above $\sim 100 \times 10^{18}$ n/cm^2 when the samples are fully amorphized. For intermediate doses the situation is more complicated [8,10,11].

ii) For small irradiation doses the amorphous volume fraction of the samples, determined by mass density measurements, is smaller than the ratio $P_{\mathrm{n-quartz}}/P_{\mathrm{glass}}$ where $P_{\mathrm{n-quartz}}$ and P_{glass} denote the density of states of tunneling states in neutron-irradiated quartz and in vitreous silica, respectively. This was interpreted as a clear indication that tunneling states do not only reside in the amorphous clusters but also in the disturbed crystalline regions [7,12].

iii) Using different crystal cuts of neutron-irradiated quartz a strong anisotropy of the coupling between phonons and tunneling states was observed. This gave further evidence for the existence of tunneling states in the slightly disordered crystalline regions. Moreover, it led to a microscopic picture of the tunneling states in the crystalline regions [9]. It was suggested that the tunneling states are related to the radiation-induced occurrence of so-called

* This paper is dedicated to Prof. H. Horner on occasion of his 60th birthday.

[a] e-mail: classen@urz.uni-heidelberg.de

α_1-α_2- or Dauphiné-twins. These twins consist of groups of SiO_4-tetrahedra which are rotated 180° with respect to each other around the optical axis (*i.e.* the z-axis). Small displacements of approximately 0.4 Å of tetrahedra chains are sufficient to move from the original α-configuration to the opposite one. The rigid tetrahedra remain basically unchanged as no breaking of bonds is required for this motion.

In the present paper we show and discuss results of *low-frequency* elastic (vibrating reed) measurements on unirradiated quartz and on quartz samples irradiated with five different neutron doses. We hereby extend the range of temperatures and frequencies for investigations of the elastic properties of neutron-irradiated quartz quite considerably. Only very few low-frequency measurements have been carried out until now [13] and except for some phonon echo measurements [14] no elastic measurements at all below 0.3 K. The motivation for the present study arises from several open questions.

It is known that in glasses the distribution functions of relaxation times and energies extend over many orders of magnitude. Due to the lack of low frequency and very low temperature measurements on neutron-irradiated quartz, however, only a rather narrow window of relaxation times and energies has been investigated so far for these disordered solids. Hence it is not yet known whether or not the distribution functions are as broad as in glasses. Measurements at low frequencies may reveal new information on tunneling states with long relaxation times, while experiments at very low temperatures are a probe of tunneling systems with very small energy splittings.

A second substantial motivation for experiments at very low temperatures results from the improved understanding of the relevance of interaction among tunneling states. There is clear experimental evidence that at very low temperatures the dynamic properties of glasses are strongly influenced by the mutual interaction between tunneling states and not only by the interaction of tunneling states with phonons [15–20]. Hence the question arises if in a solid like neutron-irradiated quartz, that contains very likely defects of similar nature as vitreous silica but in smaller number, interaction between tunneling states is less important. It appears be to a promising idea to "tune" the interaction between tunneling states by a variation of the neutron dose.

Finally, our measurements are intended as an independent test of the above mentioned anisotropy of the coupling between tunneling states and phonons that has been demonstrated so far solely by means of ultrasonic experiments. The interesting microscopic implications of this observation make it worthwhile to reexamine the elastic properties of neutron-irradiated quartz using a different experimental technique. A brief account of some of the results has been given elsewhere [21].

The paper is organized as follows: In Section 2 we will briefly recall some predictions of the tunneling model that is widely used as a baseline of discussion of the low-temperature acoustic properties of amorphous solids. In addition, we will mention several shortcomings and necessary extensions of this model. Section 3 gives some information on the experimental technique and on the sample specification, while Section 4 contains the presentation and discussion of our experimental results.

2 Theory

2.1 Standard tunneling model

In this section we briefly summarize the assumptions and predictions of the tunneling model that are relevant to low-frequency acoustic experiments. For more detailed discussions see, *e.g.*, references [22,23]. The basic assumptions of the tunneling model are:

i) In amorphous solids some atoms or small groups of atoms can move between two almost degenerate configurations in double well potentials with asymmetry Δ and tunnel splitting $\Delta_0 \simeq E_0 \exp(-\lambda)$. Here E_0 is the ground state energy in a single well and $\lambda \simeq d\sqrt{2mV}/2\hbar$ the tunneling parameter which is determined by the distance d in configurational space between the two potential minima, the mass m of the "particle", and the barrier height V between the wells. The total energy splitting between the two lowest levels is given by $E = \sqrt{\Delta^2 + \Delta_0^2}$.

ii) The parameters Δ and λ are independent of each other and they are widely distributed because of the randomness of the local environment. Usually, a distribution function

$$P(\Delta, \lambda)\mathrm{d}\Delta\mathrm{d}\lambda = \overline{P}\mathrm{d}\Delta\mathrm{d}\lambda \tag{1}$$

is assumed where $\overline{P}$ is a constant.

iii) At temperatures below 1 K the dominant relaxation mechanism for tunneling systems in insulators is the so-called one-phonon or direct process. The rate of this process is given by [24]

$$\tau_\mathrm{d}^{-1} = \frac{1}{2\pi\rho\hbar^4}\left(\frac{\gamma_\mathrm{l}^2}{v_\mathrm{l}^5} + \frac{2\gamma_\mathrm{t}^2}{v_\mathrm{t}^5}\right)\Delta_0^2 E \coth\frac{E}{2k_\mathrm{B}T} \tag{2}$$

where ρ is the mass density, v the sound velocity, and $\gamma = (1/2)\mathrm{d}\Delta/\mathrm{d}e$ the deformation potential, *i.e.*, the derivative of the asymmetry energy with respect to strain e. Indices l and t in equation (2) denote longitudinal and transversal polarization, respectively. For a given energy splitting, there is a wide distribution of relaxation times, and amongst this distribution symmetric tunneling systems ($E = \Delta_0$) have the shortest relaxation times, denoted by τ_min.

Using these assumptions the following predictions for the temperature dependence of the internal friction Q^{-1} and for the relative change of sound velocity $\delta v/v$ of an insulating glass below 1 K are obtained:

At low temperatures, when $\omega\tau_\mathrm{min} \gg 1$, the internal friction increases as the third power of temperature, and the sound velocity is expected to vary logarithmically with temperature as

$$\frac{\delta v}{v} = C\ln\left(\frac{T}{T_0}\right) \tag{3}$$

where T_0 is an arbitrary reference temperature, and the parameter C is given by $C = \overline{P}\gamma_i^2/\rho v_i^2$; the index i stands for longitudinal or transversal polarization.

At higher temperatures, when $\omega\tau_{\min} \ll 1$, the internal friction approaches the value

$$Q^{-1} = \frac{\pi}{2}C \tag{4}$$

independent of temperature and frequency. The sound velocity passes a maximum and then decreases logarithmically with increasing temperature as

$$\frac{\delta v}{v} = -\frac{C}{2}\ln\left(\frac{T}{T_0}\right). \tag{5}$$

For the position $T_{\max}$ of the maximum of sound velocity one obtains

$$T_{\max} = \sqrt[3]{\frac{\pi\rho\hbar^4\omega}{k_{\mathrm{B}}^3}\left(\frac{\gamma_{\mathrm{l}}^2}{v_{\mathrm{l}}^5} + \frac{2\gamma_{\mathrm{t}}^2}{v_{\mathrm{t}}^5}\right)^{-1}}. \tag{6}$$

Hence by measuring $T_{\max}$ one can obtain information on the deformation potential γ. Here γ denotes an average over all directions and polarizations of thermal phonons. From equations (3–5) it becomes clear that the parameter C may be considered as a "macroscopic coupling constant" which determines the integral influence of the tunneling states on the low-temperature elastic properties. One should mention that C varies only within one order of magnitude for virtually all glasses even though they may have completely different structure, chemical composition, and type of bonding. An exception of this "universality" was found recently [25].

2.2 Extensions and modifications of the standard tunneling model

Over the past years the standard tunneling model has been proven to provide a fairly good description of the low-temperature properties of amorphous solids and is therefore generally accepted as an adequate, though purely phenomenological, approach. However, a closer look reveals that the agreement between theory and experiments is not truly satisfactory, in particular at very low temperatures ($T < 0.1$ K) and at temperatures above ~ 1 K. The reason for the shortcomings of the standard model is that the nature of the tunneling process changes both at very low and at elevated temperatures as will be discussed in the following paragraphs.

2.2.1 Temperatures above 1 K

At temperatures above a few Kelvin, the sound velocity no longer obeys equation (5) but changes from a logarithmic to an approximately linear temperature dependence, and the internal friction exhibits a strong increase with increasing temperature above ~ 5 K [23,26,27]. In this temperature range the number of phonons becomes so large that relaxation does no longer occur predominantly via the one-phonon process; the probability of more complicated relaxation processes increases.

At temperatures above ~ 1 K two-phonon (Raman) relaxation processes may occur; they lead to a stronger decrease of $\delta v/v$ with increasing temperature but do not change the plateau region of the internal friction.

At yet slightly higher temperatures, the large thermal fluctuations may lead to incoherent tunneling, *i.e.* to the destruction of the phase coherence of the tunneling motion [28]; this may have a considerable influence on the dynamic properties of disordered solids. Fair agreement with experimental observations is obtained by taking into account this effect [27].

Finally, above $\sim$ 5–10 K in glasses relaxation may be described as classical Arrhenius type hopping over the barrier of the double well potentials [29] with a rate

$$\tau_{\mathrm{th}}^{-1} = \nu_0 \exp\left(-\frac{V}{k_{\mathrm{B}}T}\right). \tag{7}$$

Here ν_0 denotes an attempt frequency supposed to be on the order of the Debye frequency.

It is extremely difficult to take all possible effects at higher temperatures adequately into account. In the simplest approximations Raman processes and incoherent tunneling are neglected and it is assumed that the total relaxation rate is simply given by the sum of the one-phonon rate (Eq. (2)) and the rate τ_{th}^{-1} (Eq. (7)) of classical thermally activated relaxation. Tielbürger *et al.* [26] proposed a Gaussian distribution function of width V_0 for the barrier heights

$$P(\Delta, V) = \frac{\overline{P}}{E_0}\exp\left(-\frac{V^2}{2V_0^2}\right) \tag{8}$$

which in combination with the additionally assumed correlation $\lambda \propto V$ replaces equation (1). For low temperatures ($T < 1$ K) when only systems with small barriers (or tunneling parameters) are relevant the use of equation (8) leads to the same predictions (Eqs. (3–6)) as the simple distribution function (1). At temperatures $T > E_0/2k_{\mathrm{B}}$ thermal relaxation sets in and causes an increase of the internal friction with increasing temperature and a decrease of the sound velocity which are both linear in temperature. When the temperature is raised systems with higher barriers contribute to the internal friction. However, since the width V_0 of the barrier distribution (Eq. (8)) is finite the internal friction does not further increase but passes a maximum and decreases afterwards with increasing temperature. The position and the height of the maximum of Q^{-1} are approximately proportional to V_0. These predictions are in fair although not perfect quantitative agreement with experimental observations made on several glasses [23,26,27].

A distribution function $P(V)$ different from equation (8) is used in the so-called "soft potential model" [30] which is based on a more general approach for the potentials of the defect systems and also includes contributions from quasiharmonic low-energy excitations.

The soft potential model gives qualitatively similar but quantitatively slightly different predictions for the thermally activated regime. Based on the assumptions regarding the potential parameters a distribution function $P(V) \propto V^{-\alpha}$ is predicted for small values of the barriers, where α is a number between 0.25 and 0.75 depending on the glass. We will briefly come back to this point in Section 4.1 but we will refrain from a detailed discussion of the soft potential model in this paper.

2.2.2 Temperatures below 0.1 K

Low-frequency acoustic measurements on several glasses [23,27] show clear deviations from the predictions of the standard tunneling model also at very low temperatures. For instance, the ratio of slopes of the change of sound velocity below and above the maximum was found to be rather close to $1 : (-1)$ rather than $2 : (-1)$ as expected from equations (3, 5). Moreover, below a few millikelvin a "cutoff" or "saturation" of the sound velocity occurs, *e.g.* in vitreous silica [31], and the internal friction varies at very low temperatures almost linearly in temperature rather than proportional to T^3 [23,27,31]. These and several other experimental results [15–17,20] indicate that the standard picture of non-interacting tunneling states is not sufficient but that interaction between tunneling states can be of great importance, in particular at very low temperatures.

Various theories have been suggested to take into account the mutual interaction of tunneling states in glasses [32–34]. Recently, Burin and Kagan [35] proposed the occurrence of pair excitations due to interacting tunneling states to explain the linear temperature dependence of the internal friction in glasses at very low temperatures.

A somewhat different approach to address the above mentioned experimental results was given by two of us [19]. Based on a theory worked out by Würger for the tunneling of substitutional defects in alkali halides [36,37] a simplified picture for the possible influence of interaction between tunneling states in glasses was developed. In this model the interaction leads to an incoherence of the tunneling motion at very low temperatures. As a result, the resonant contribution to $\delta v/v$ is reduced but additional relaxation effects occur and modify the temperature dependence of $\delta v/v$ and Q^{-1}. For instance, the temperature dependence of the internal friction at low temperatures changes from a cubic to an approximately linear behavior [19].

3 Experimental

3.1 Vibrating reed technique

The low-frequency elastic properties of small plates or reeds can be investigated using the vibrating reed technique [23,31,38]. A thin rectangular plate of the sample material is clamped at one end between two copper blocks. Before clamping, a thin ($\sim$ 30 nm) gold film is sputter-deposited on both sides of the reed to provide electric conductivity. The reed is electrostatically driven to forced vibrations at its lowest eigenfrequency by an electrode close to the sample surface at the free end, and a second electrode on the opposite side is used for the detection of the vibration. Typical resonance frequencies are in the range 1−10 kHz.

A phase-sensitive detection scheme and computer-based control loop is used to keep the sample at resonance. Relative changes of the sound velocity $\delta v/v = \delta f/f$ can be measured with an accuracy better than 10^{-6} by monitoring changes of the resonance frequency f. The absolute value of the internal friction Q^{-1} is determined with an accuracy of 3−5% from evaluation of full resonance curves or from the exponential decay of the vibrational amplitude after turning off the drive voltage. The best resolution for the detection of relative changes of the internal friction with a typical error of 1% is achieved by monitoring $\delta A/A \simeq \delta Q/Q$, where A is the amplitude of the reed at resonance.

As especially at low temperatures spurious nonlinear behavior of the reeds may occur, *i.e.*, a dependence of the resonance frequency and/or the internal friction on the drive voltage [23,31], attention was paid to ensure that the resonance curves were always symmetric. The maximum strain amplitudes occurring at the clamping position were 1×10^{-7} or less. Only for sample K17 (100×10^{18} n/cm^2) some nonlinear behavior remained as in this measurement the signal-to-noise ratio at very low temperatures was too small to allow a further reduction of the excitation voltage.

Another problem of vibrating reed experiments are background losses due to sample clamping which impose a severe limit on exact measurements of very small values of the intrinsic internal friction and of very small changes of the sound velocity. This background contribution that seems to vary in a non-universal way for different samples makes it difficult to interpret results in the high-Q regime ($Q \sim 10^5$ and above) of vibrating reeds quantitatively. The underlying physical reasons of background losses are only poorly understood yet. It seems plausible that some vibrational energy of the reed is transferred into the copper clamps since at the clamping position the maximum strain amplitudes occur; this "radiation" effect would lead to a finite dissipation even if the intrinsic losses of the sample were negligibly small. It is still not clear, however, to which extent the observed changes of $\delta v/v$ and Q^{-1} are determined by the acoustic mismatch between reed and clamp, by the internal friction of the clamp material, or by the intrinsic properties of the sample. We want to stress, however, that the background losses become important only for samples with high quality factors Q.

3.2 Sample characterization

The reeds were cut from pieces of synthetic quartz and were irradiated with fast neutrons at SCK in Mol, Belgium. Typical sample dimensions were $8\times2\times0.2$ mm^3.

Table 1. Label, neutron irradiation dose, mass density, and resonance frequency of the samples. Relative errors of the mass density measurements of the neutron-irradiated samples are $\sim 10^{-3}$.

Label	Neutron dose [10^{18} n/cm^2]	Mass density [g/cm^3]	Frequency [kHz]
unirradiated	0	2.6499	3.1
K12	4.6	2.640	5.8
K15	21	2.631	7.6
K16	47	2.557	3.1
K17	100	2.256	3.3
K18	200	2.258	2.9

The irradiation was isotropic, and the sample temperature during irradiation was approximately 100 °C. Samples with five different irradiation doses (4.6−200 × 10^{18} n/cm^2) were studied as well as an unirradiated quartz crystal. The irradiation doses refer to the flux of neutrons with energies above 0.3 MeV. Table 1 lists the labels (which are the same as those for the ultrasonic studies of Refs. [5–11]), the neutron-irradiation doses, the mass densities, and the eigenfrequencies of all samples.

The long side (8 mm) of the reeds was parallel to the crystallographic z-axis, and the second longest side (2 mm) parallel to the x-axis. Since in a vibrating reed experiment a bending mode is excited both longitudinal and transversal strain occurs in the sample. In our geometry the longitudinal strain was parallel to the z-axis while transversal strain occurred in y-direction (and no strain at all in x-direction). The ratio of the longitudinal to the transversal strain amplitude depends on Poisson's ratio σ. For a typical value $\sigma \simeq 0.1$ the longitudinal component is about twice as large as the transverse one.

4 Results and discussion

4.1 Overall temperature dependence

Figure 1 shows the temperature dependence of the sound velocity over a wide range of more than four decades in temperature for the unirradiated quartz sample, the neutron-irradiated samples K12 and K17 (4.6 and 100 × 10^{18} n/cm^2, respectively), and, for comparison, of vitreous silica (Suprasil W, $f = 11.4$ kHz). The low-temperature ($T < 1$ K) properties of the quartz samples will be discussed in more detail in the following Section 4.2. For the overall picture it is important to note that the changes of the sound velocity of the unirradiated reed and of the K12 sample are very similar: Below 10 K the temperature dependence of the sound velocity is very small but at higher temperatures a strong reduction of $\delta v/v$ occurs which is a little more pronounced for the lightly irradiated sample. This decrease of the sound velocity with increasing temperature cannot be explained to arise only from the increase of the internal energy — in this case one would expect a reduction proportional to T^4 which is not seen

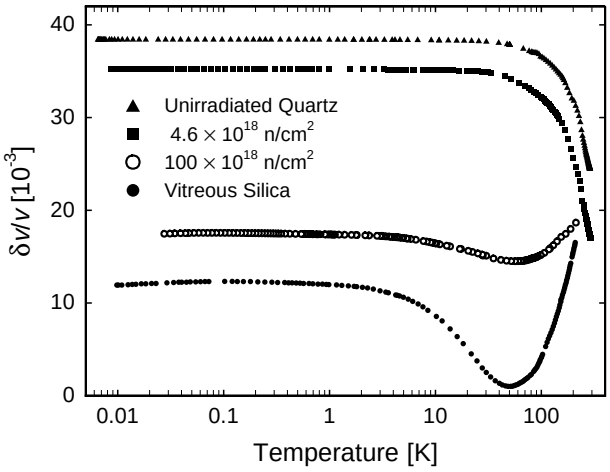

Fig. 1. Temperature dependence of the relative change of sound velocity of an unirradiated quartz crystal, of neutron-irradiated quartz samples K12 (4.6×10^{18} n/cm^2) and K17 (100×10^{18} n/cm^2), and of vitreous silica (Suprasil W). Data for different samples were offset for clarity.

in the experiments. Rather, a more complicated polynomial fit with a linear, quadratic, and quartic term leads to a satisfactory agreement with the data; however, it remains unclear, if such a fit with three free parameters has a distinct physical meaning. It is conceivable that — as recently demonstrated by Liu *et al.* [39] in low-frequency experiments on metals — dislocations have a significant influence on the elastic properties observed here.

In comparison to the lightly irradiated reed (K12), the sample K17 (100×10^{18} n/cm^2) which is in the completely amorphous metamict phase shows a qualitatively different behavior: It exhibits a minimum of sound velocity around 60 K which is also seen in vitreous silica at a similar temperature (50 K). The reason for the occurrence of this minimum that has been observed before in vitreous silica in several high frequency measurements [26,40,41] is still not clear. The point we want to make here is that highly irradiated quartz crystals show a qualitatively similar (though quantitatively different) behavior as vitreous silica whereas lightly irradiated quartz samples have very similar low-frequency elastic properties as unirradiated quartz. This confirms the expectation that by an enhancement of the neutron dose it is possible to obtain a transition from crystal-like to glass-like elastic properties; similarly, such a transition has been clearly demonstrated for the low-temperature thermal conductivity by de Goër *et al.* [42].

The general observations from Figure 1 are confirmed by measurements of the temperature dependence of the internal friction. In Figure 2 again results for sample K12 and for a sample in the metamict phase (K18, 200×10^{18} n/cm^2) are shown in comparison to vitreous silica (data from Ref. [23]). For clarity, results for the unirradiated sample have been omitted in this graph since on the coarse scale of Figure 2 they could be hardly distinguished from those of sample K12. The lightly irradiated crystal K12 has a very small internal friction

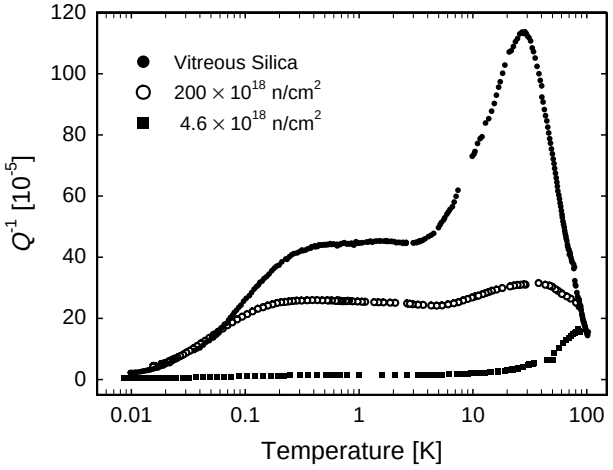

Fig. 2. Temperature dependence of the internal friction of neutron-irradiated quartz samples K12 (4.6×10^{18} n/cm^2) and K18 (200×10^{18} n/cm^2) and of vitreous silica (Suprasil W).

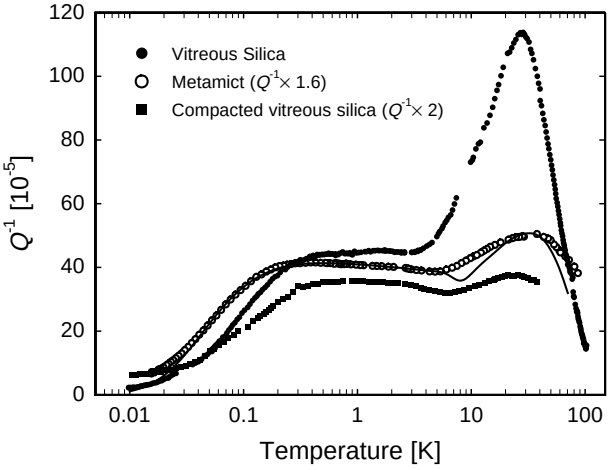

Fig. 3. Comparison between the temperature dependence of the internal friction of vitreous silica (Suprasil W), neutron-irradiated quartz in the metamict phase (K18, 200×10^{18} n/cm^2), and compacted vitreous silica (Suprasil I). Data for sample K18 were multiplied by 1.6 and data (from Ref. [43]) for the compacted glass by 2. The solid line is a fit described in the text.

and shows only a weak temperature dependence below 10 K. At higher temperatures the internal friction increases and becomes around 100 K comparable to the values of the other two samples shown in Figure 2.

Qualitatively and quantitatively completely different are the data for vitreous silica which can be well described by the theory depicted in Section 2 (see also Refs. [23,26]). Around 1 K the internal friction is almost independent of temperature as predicted by equation (4). Above 5−10 K thermally activated relaxation and/or incoherent tunneling [27] set in and lead to an increase of Q^{-1} whereas above 30 K the internal friction decreases due to the decreasing number of double well potentials with large barriers. At temperatures below $\sim$ 200 mK the internal friction decreases with decreasing temperature since the relaxation times even of the fastest tunneling systems with $E \simeq k_{\rm B}T$ become too long to fulfill $\omega\tau_{\rm min} = 1$.

The irradiated quartz K18 shows a similar qualitative behavior as the glass but several interesting differences between the two samples can be observed. First of all, the plateau value of the internal friction of sample K18 is approximately 40% smaller than for vitreous silica. This is remarkable since both samples are fully amorphous, have the same chemical composition, and are constituted of the same basic unit, namely the SiO_4 tetrahedron. A similar result has been found in ultrasonic measurements on samples K17 [8] and, very recently, K18 [11]. Secondly, in the "plateau" region the internal friction is not really independent of temperature but a small decrease of Q^{-1} with increasing temperature occurs. Finally, the maximum of Q^{-1} of the metamict sample around 30 K is reduced by more than a factor of 3 compared to vitreous silica. These observations indicate that the distribution of the characteristic parameters of the tunneling states in both samples must be significantly different; a simple scaling of the distribution function of vitreous silica by a constant factor is not sufficient to explain the data of sample K18. The fact that Q^{-1} is not independent of temperature in the plateau region points to a distribution function which, in contrast to equation (8), is not constant even for small potential barriers V or tunneling parameters λ. Moreover, the strong suppression of the thermal relaxation peak indicates that the reduction of systems with high barriers is more pronounced than that of defect states with low barriers. A numerical analysis shows that fair agreement between data and theory can be obtained by multiplying the distribution function (8) by a term const$\times V^{-0.3}$ as shown in Figure 3 by the solid line. Significant deviations occur only in the temperature ranges below 50 mK (see Sect. 2.2.2), around 10 K (see Sect. 2.2.1), and above 50 K where apparently the assumed distribution function $P(V)$ drops off too quickly. One should note that the additional term $V^{-0.3}$ in the barrier distribution is in good agreement with the soft potential model briefly mentioned in Section 2.2.1 and deviates from the assumption of the standard tunneling model (Eq. (1)).

What are the reasons for the differences between the glassy and the metamict phase of SiO_2? One obvious difference between the samples is the density which is approximately 3% smaller in the glass (2.20 *vs.* $\sim$ 2.26 g/cm^3). It appears therefore interesting to compare our results with internal friction data of *compacted* vitreous silica which were obtained with the same experimental technique [43]. The sample was a piece of Suprasil I glass [44] densified at 600 °C and at a pressure of 40 kbar. The resulting mass density was 2.45 g/cm^3, *i.e.*, about 11% higher than before densification. Figure 3 shows the temperature dependence of the internal friction of this sample at 12 kHz in comparison with the neutron-irradiated quartz K18 and vitreous silica (same data as in Fig. 2). Note that in Figure 3 the data (open circles) and the fit (solid line) of the K18 sample were multiplied by 1.6 and the data of the compacted sample (filled squares) by a factor of two. This was done to scale the plateau regions

of all three samples to a similar — though still distinguishable — level and thus to demonstrate that the heights of the relaxation peaks around 30 K scale in a clearly different way than the plateaus around 1 K. Figure 3 demonstrates that the compacted sample has a "plateau" value of Q^{-1} which is almost 30% and a relaxation peak which is more than 40% smaller than for the metamict sample. Comparing the results of the three samples we find a systematic correlation: Firstly, an increase of the mass density of amorphous SiO_2 leads to an overall reduction of the density of states of double well defect states and secondly, the shape of the barrier distribution function changes — an increase of ρ reduces the number of defect states with high barriers more drastically than the number of systems with small barriers.

The results of Figure 3 also allow a comparison of the coupling strengths γ — or more precisely, of the prefactors of the one-phonon relaxation rate (Eq. (2)) — as the plateau region will extend to lower temperatures when γ is enhanced. It turns out that the prefactors of the one-phonon relaxation rate have very similar values for all three samples. The differences in the low-temperature part of the curves — the plateau of Q^{-1} of the metamict sample extends to significantly lower temperatures — are only a consequence of the smaller experimental frequency of this sample (2.9 kHz *versus* 11.4 and 12 kHz, respectively).

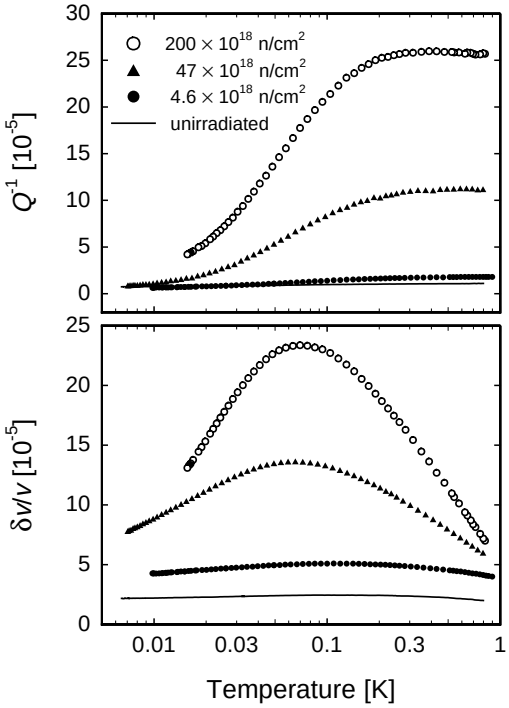

Fig. 4. Temperature dependence of the internal friction (upper panel) and of the relative change of sound velocity (lower panel) below 1 K of an unirradiated quartz crystal (solid line) and of neutron-irradiated quartz samples K12, K16, and K18 (from bottom to top). Sound velocity data for different samples were offset for clarity.

4.2 Low-temperature properties

4.2.1 Temperature dependence

The range of very low temperatures ($T < 1$ K) reveals in general particularly interesting information on the number and the dynamics of tunneling states in disordered solids (Eqs. (3–6)). Figure 4 shows the temperature dependence of the internal friction (upper panel) and of the relative change of sound velocity (lower panel) below 1 K of the unirradiated quartz crystal (solid line) and of neutron-irradiated quartz samples K12, K16, and K18 (from bottom to top). Note that the ordinate of the sound velocity panel is expanded by more than two orders of magnitude compared to Figure 1 and the ordinate of the internal friction panel by a factor of four compared to Figure 2. In contrast to the overall temperature behavior, all samples show a qualitatively similar low-temperature behavior but drastic quantitative differences occur. At the lowest temperatures the sound velocity increases as the logarithm of temperature, passes a maximum, and decreases towards higher temperatures, again nearly logarithmically. The internal friction increases strongly with rising temperature and becomes almost independent of temperature above a few 100 mK (plateau region). These findings are in qualitative agreement with the predictions of the tunneling model equations (3–5) but, quite remarkably, all deviations that have been observed in recent measurements on glasses [23,27,31] (see Sect. 2.2.2) can be observed for the neutron-irradiated quartz crystals as well: The ratio of slopes of the sound velocity below and above the maximum is close to $1 : (-1)$ rather than $2 : (-1)$ and the internal friction increases approximately linearly rather than as the temperature cubed. Thus if we follow reference [19] and assume that like in glasses the shortcomings of the tunneling model are due to the neglection of interaction among the tunneling states we are led to conclude that in neutron-irradiated quartz crystals interaction between neighboring tunneling systems is of great importance, too. This may impose interesting microscopic implications: As mentioned in the introduction the radius of the radiation-damaged regions in quartz is only on the order of 10 Å. If interaction between tunneling states is important even for lightly irradiated samples like K12 where most amorphous clusters are still well separated this seems to imply that a single cluster — including, however, its disturbed crystalline environment — would have to host more than one tunneling system. Interaction between tunneling systems in different clusters appears to be a less favorable explanation since an increase of the cluster density (*i.e.* of the neutron dose) does not lead to a qualitative change of the temperature dependence of the elastic properties.

However, the above interpretation has to be considered with some caution since the experimental results may be influenced by background losses arising from the sample clamping (see Sect. 3.1). In particular, the results for sample K12 that has a very small internal friction may be affected to some extent by these background effects.

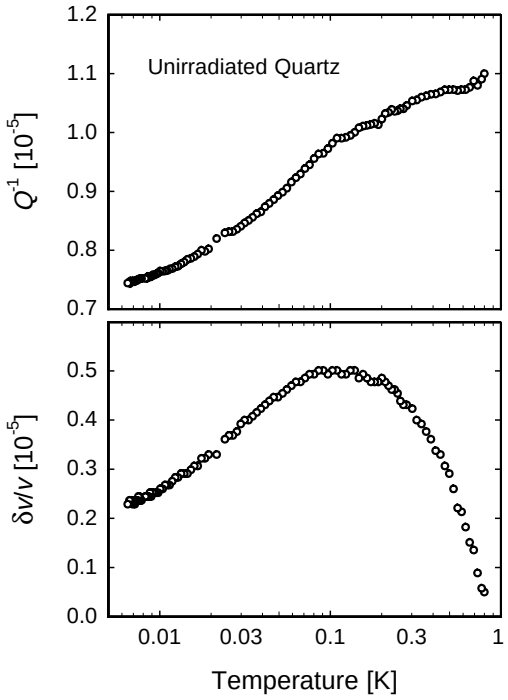

Fig. 5. Temperature dependence of the internal friction (upper panel) and of the relative change of sound velocity (lower panel) below 1 K of the unirradiated quartz sample.

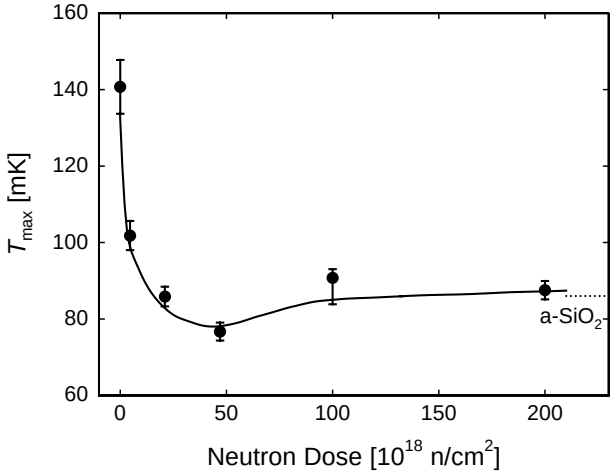

Fig. 6. Temperature $T_{\max}$ at which the maximum of sound velocity occurs as a function of the neutron dose. To allow a reasonable comparison between the different measurements which were all taken at different frequencies, all data points were scaled using equation (6) to a typical frequency of 5 kHz. The dotted line labeled a-SiO_2 indicates the corresponding maximum temperature for vitreous silica [23]. The solid line is a guide to the eye only.

As an example of the possible relevance of background contributions we show in Figure 5 the data of the unirradiated quartz sample on a scale that was expanded once more by almost a factor of 50 compared to Figure 4. Although the sound velocity data show a behavior somewhat different from that of the irradiated crystals — the slope of $\delta v/v$ below the maximum is clearly smaller than above the maximum — there is still an overall qualitative similarity. In contrast, ultrasound experiments showed below 10 K no significant temperature dependence of the sound velocity of a sample cut from the same piece of material [7] and measurements of the ultrasound attenuation were limited by the experimental resolution, *i.e.*, the attenuation of the sample was extremely small [6].

Although a conclusive statement on the relevance of interaction for lightly irradiated quartz samples cannot be made we want to stress that (with the possible exception of sample K12) the data for the neutron-irradiated samples (K15 – K18) are barely influenced by background losses since the intrinsic relaxation contributions are considerably larger than all spurious effects.

4.2.2 Dependence on the neutron dose

It is interesting to have a closer look at the positions of the maximum of sound velocity of the different samples (see Figs. 4 and 5). According to equation (6) the temperature of the maximum is closely related to the prefactor of the one-phonon relaxation rate (Eq. (2)) and thus to the deformation potential. With increasing dose the maximum first shifts to lower temperatures (130 mK for the unirradiated crystal, 110 mK for sample K12, and 65 mK for sample K16) but then for even higher irradiation doses the temperature of the maximum slightly increases (70 mK for sample K18). Unlike in the discussion of the internal friction data of Figure 3 at the end of Section 4.1, these differences cannot be solely explained by the different experimental frequencies. To eliminate the effects due to the different measuring frequencies we have assumed the relation $T_{\max} \propto \omega^{1/3}$ (Eq. (6)) to be valid for our experiments and have scaled all experimental values $T_{\max,\exp}$ to the same reference frequency $f_{\rm ref} = 5$ kHz, *i.e.*, $T_{\max,\rm scaled} = T_{\max,\exp}(f_{\rm ref}/f)^{1/3}$. The results for all samples are shown in Figure 6 as a function of the neutron dose. As already indicated above, for the sample K16 a shallow minimum of $T_{\max}$ occurs indicating a particularly strong coupling γ between tunneling systems and phonons for this sample. We will discuss this observation in some more detail in the following subsection 4.3. The rather large lower error bar of sample K17 (100×10^{18} n/cm^2) is a result of nonlinear behavior that could not be entirely avoided for this sample (see Sect. 3.1). It is known from glasses that in the nonlinear range of vibrational amplitudes the position of the maximum shifts to higher temperatures when the drive voltage is increased [23,31].

From Figure 4 and from similar data for the reeds K15 and K17 one can deduce the macroscopic coupling constants C for the different samples using equations (3–5). However, as the experimental results, *e.g.* the ratio of slopes of $\delta v/v$ below and above the maximum, cannot be correctly described by the standard tunneling model the parameters C will have different values depending on whether equation (3), (4), or (5) is used. On the other hand, all samples show very similar deviations

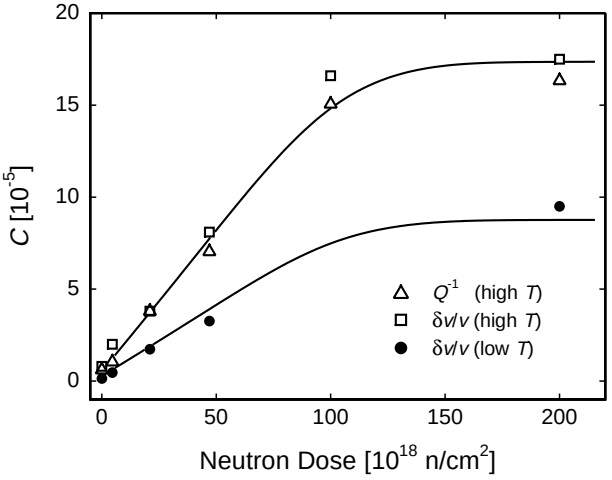

Fig. 7. "Macroscopic coupling constants" C for all samples investigated. Open triangles denote data where C was derived from the plateau value of Q^{-1} (Eq. (4)) while the open squares (full circles) were derived from the slope of the sound velocity above (below) the maximum of sound velocity (Eqs. (3, 5)). Error bars ($\sim$ 6% for Q^{-1} and $\sim$ 10% for $\delta v/v$) have been omitted for clarity. The solid lines are guides to the eye only.

from the standard tunneling model and hence it may still be interesting to discuss the values of the macroscopic coupling constants determined from different methods as a function of neutron dose. Moreover, as discussed in Section 2.2, one may expect that the standard tunneling model gives a reasonable quantitative description at least at temperatures $\sim 0.2 - 1$ K where equations (4, 5) are applicable. Figure 7 shows different data sets of C as a function of neutron dose where C was determined from the low-temperature slope of the sound velocity according to equation (3) (full circles), from the "high-temperature" ($T > 250$ mK) slope of $\delta v/v$ according to equation (5) (open squares), and from the plateau value of the internal friction according to equation (4) (open triangles). The latter two sets of data are in good agreement whereas — corresponding to the "wrong" ratio of slopes — the values of C determined from the low-temperature slope of $\delta v/v$ are smaller by approximately a factor of two. However, all data sets show almost the same relative change of C as the neutron dose is enhanced: C increases approximately linearly for small and moderately high doses ($\leq 50 \times 10^{18}$ n/cm^2) and saturates for high doses ($\geq 100 \times 10^{18}$ n/cm^2). Only a very small change of C is observed when the dose is increased from 100×10^{18} n/cm^2 to 200×10^{18} n/cm^2. This is not surprising since sample K17 (100×10^{18} n/cm^2) is known to be already completely amorphous, and hence only minor structural changes will be induced upon further irradiation. No value of C was determined for sample K17 from the low-temperature slope of the sound velocity. Again the reason was that the low-temperature results for this specimen were significantly influenced by nonlinearities which lead to systematic errors in $\delta v/v$ [23,31].

4.3 Comparison with ultrasound experiments

It is interesting to compare the results of Figure 7 with data derived from experiments where longitudinal ultrasound was applied to neutron-irradiated quartz samples cut along different crystal axes. The investigated samples in the present work are from the same origin as those used in the ultrasound measurements. In addition, the samples were irradiated in the same reactor, using the same irradiation procedure and the same flux calibration. This makes reliable comparisons possible. Comparisons between data from different reactor sites cannot readily be made because of differences in flux calibration procedures. Figure 8 shows the parameter C derived from ultrasound attenuation measurements for crystals cut in x- (open squares) [8,10] and in z-direction (full circles) [9] in comparison to our data derived from the plateau value of the internal friction (open circles). The data point (open square) at 200×10^{18} n/cm^2 was actually deduced from sound velocity measurements and appropriately scaled to allow for the differences in the values of C determined from $\delta v/v$ and Q^{-1}, respectively [11]. Although the K18 sample (200×10^{18} n/cm^2) was a x-cut crystal one expects the same result for a z-cut quartz irradiated with this high dose since the sample should be completely isotropic. Therefore the guiding line for the z-cut samples extends to 200×10^{18} n/cm^2.

As mentioned in the introduction a strongly anisotropic behavior is found in the ultrasound experiments. While the results for the z-cut samples — a monotonic increase for small doses and a saturation at high doses — are fairly close to the vibrating reed data, the x-cut samples exhibit a pronounced maximum of C at a dose of 47×10^{18} n/cm^2. This strong anisotropy has been interpreted to arise from the anisotropy of the tunneling motion of two-level-systems in the crystalline regions of the sample (see introduction) [9]. Similar ideas for the microscopic origin of the tunneling states in vitreous silica have tentatively been proposed by other groups [45,46]. In fact, it seems very plausible that the nature of the tunneling states in amorphous SiO_2 is not much different from that in the distorted crystalline regions of neutron-irradiated quartz.

The monotonic dose dependence of C observed in our vibrating reed measurements is consistent with the ultrasound data and hence with the underlying microscopic picture. In our experiments the dominant strain component is longitudinal and parallel to the z-axis. Hence we may expect that the values of C derived from the low frequency experiments are similar to those for the ultrasound experiments on z-cut samples. Despite the very large difference (factor 10^5) in experimental frequency — and thus in relaxation times of the relevant tunneling systems — the results do in fact agree even quantitatively within $\sim 30\%$. This demonstrates, in accordance with former low-frequency elastic measurements [13], that the distribution of relaxation times must be similarly broad as for amorphous solids.

One may wonder whether one would not expect at least a small anomaly in Figure 7 for the sample K16

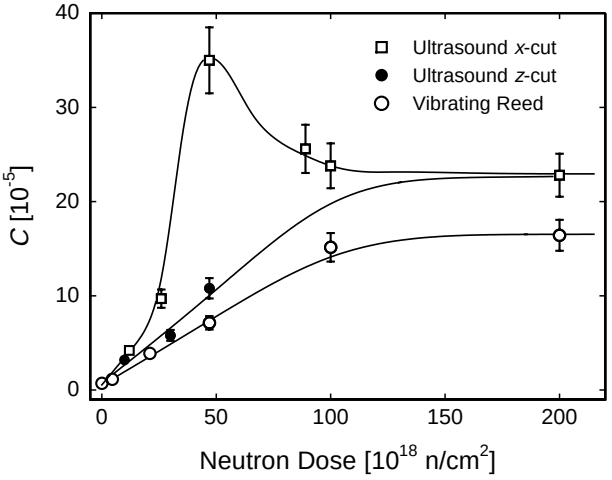

Fig. 8. "Macroscopic coupling constants" C as a function of the neutron dose. Open circles denote data derived from vibrating reed measurements of the plateau height of Q^{-1} (same data as in Fig. 7). Also shown are the values of C derived from ultrasound experiments for crystals cut in x- (open squares) and in z-direction (full circles) (from Ref. [11]). The solid lines are again only guides to the eye.

(47×10^{18} n/cm^2), since besides the dominant longitudinal strain in z-direction a smaller transversal strain component perpendicular to the z-axis occurs which might contribute significantly to the elastic properties. This transversal strain, however, is for our sample geometry parallel to the y-axis and hence it is difficult to relate our results to the ultrasonic experiments; no ultrasound measurements have been performed yet in y-direction.

Even though the parameter C does not show any peculiarity for the K16 reed (47×10^{18} n/cm^2) we find an indirect indication of a directional dependence of the deformation potential when we return to the results of Figure 6: The minimum of $T_{\max}$ for sample K16 indicates a particularly strong coupling γ between tunneling states and phonons for this sample. Since thermal phonons of all polarizations and directions can contribute to the relaxation processes, the deformation potential relevant here is an average over all directions. Despite this averaging, a small effect — presumably arising from the very strong coupling of thermal phonons propagating in x-direction — remains for the highly twinned sample K16 and leads to the observed reduction of the maximum temperature of $\delta v/v$. This clearly supports the results (Fig. 8) and the interpretation of the high frequency experiments [9]. To further investigate the strong anisotropy of the phonon coupling observed in the ultrasound experiments we are planning to do vibrating reed and torsional oscillator measurements on neutron-irradiated quartz samples cut along different crystal axes.

5 Summary

We have presented a systematic investigation of the low-frequency elastic properties of neutron-irradiated quartz crystals. It was shown that the overall temperature dependence — spanning more than four orders of magnitude in temperature — of the elastic properties of the samples changes from a crystal-like to a glass-like behavior when the neutron dose is enhanced. However, even for the completely amorphized samples the density of states of tunneling systems is reduced compared to vitreous silica. All this is in agreement with previous findings in ultrasound and thermal conductivity measurements which were, however, mainly limited to the temperature region below ~ 10 K. In addition, it was found that the occurrence of double well potentials with large barriers is more strongly suppressed than that of systems with small barriers, *i.e.*, the distribution functions of double well parameters of vitreous silica and neutron-amorphized quartz are even qualitatively different. The number and the distribution of defect states seems to be closely related to the mass density or, in other words, to the free volume [47] of amorphous SiO_2 samples: Pressure compacted vitreous silica with a yet higher mass density shows an even stronger reduction of the number of defect states, especially of those with large barriers. In amorphous SiO_2 a smaller density and hence a more open structure seems to facilitate the occurrence of tunneling processes and thermally activated motions. This is not implausible since a higher mass density may lead to additional constraints in the amorphous network and may thus hinder small configurational changes.

At low temperatures the samples showed a rather similar qualitative behavior of $\delta v/v$ and Q^{-1} but very large quantitative differences. Evidence for the importance of mutual interaction of tunneling states was found for the samples irradiated with rather high neutron doses; due to limitations of the experimental method some uncertainty remained whether or not this is the case for samples with small irradiation doses, too. From the low-temperature data the macroscopic coupling constant C was determined. It showed a linear increase for small doses and a saturation when the samples become fully amorphous. A non-monotonic behavior was found for the position of the sound velocity maximum as a function of neutron dose. The sample with the largest number of Dauphiné-microtwins showed an especially strong coupling between tunneling states and phonons. This supports the microscopic picture deduced from ultrasound experiments that the tunneling motions in SiO_2 are due to coupled rotations of SiO_4 tetrahedra.

We would like to thank V. Keppens for helpful discussions. We are also grateful to G. Weiss for providing the data of the compacted glass sample and to the SCK (Mol, Belgium) for the neutron irradiation.

References

1. See, *e.g.*, *Amorphous Solids — Low Temperature Properties*, edited by W.A. Phillips (Springer, Berlin, 1981).
2. R. Comes, M. Lambert, A. Guinier, in *Interaction of Radiation with Solids*, edited by A. Bishay (Plenum Press, New York, 1967).

3. D. Grasse, O. Kocar, H. Peisl, S.C. Moss, B. Golding, Phys. Rev. Lett. **46**, 261 (1981).
4. D. Grasse, J. Peisl, B. Dorner, Nucl. Instr. Meth. B **1**, 183 (1984).
5. C. Laermans, Phys. Rev. Lett. **42**, 250 (1979); A. Vanelstraete, C. Laermans, Phys. Rev. B **38**, 6312 (1988); V. Keppens, C. Laermans, Phys. Rev. B **51**, 8602 (1995); V. Keppens, C. Laermans, M. Coeck, Nucl. Instr. Meth. B **116**, 511 (1996).
6. C. Laermans, A. Vanelstraete, Phys. Rev. B **35**, 6399 (1987).
7. A. Vanelstraete, C. Laermans, Phys. Rev. B **42**, 5842 (1990).
8. V. Keppens, C. Laermans, Nucl. Instr. Meth. B **91**, 346 (1994).
9. C. Laermans, V. Keppens, Phys. Rev. B **51**, 8158 (1995).
10. E. Peeters, C. Laermans, D.A. Parshin, M. Coeck, Nucl. Instr. Meth. B **141**, 634 (1998).
11. V. Keppens, C. Laermans, Physica B **263-264**, 149 (1999).
12. A.C. Anderson, J.A. McMillan, F.J. Walker, Phys. Rev. B **24**, 1124 (1981).
13. A. Vanelstraete, C. Laermans, L. Lejarraga, M.V. Schickfus, S. Hunklinger, Z. Phys. B **70**, 19 (1988).
14. B. Golding, J.E. Graebner, in *Phonon Scattering in Condensed Matter*, edited by H.J. Maris (Plenum Press, New York, 1980).
15. W. Arnold, S. Hunklinger, Solid State Commun. **17**, 833 (1975).
16. J.E. Graebner, B. Golding, Phys. Rev. B **19**, 964 (1979).
17. D. Salvino, S. Rogge, B. Tigner, D.D. Osheroff, Phys. Rev. Lett. **73**, 268 (1994); S. Rogge, D. Natelson, D.D. Osheroff, Phys. Rev. Lett. **76**, 3136 (1996); D. Natelson, D. Rosenberg, D.D. Osheroff, Phys. Rev. Lett. **80**, 4689 (1998).
18. A.L. Burin, J. Low Temp. Phys. **100**, 309 (1995).
19. C. Enss, S. Hunklinger, Phys. Rev. Lett. **79**, 2831 (1997).
20. P. Strehlow, C. Enss, S. Hunklinger, Phys. Rev. Lett. **80**, 5361 (1998).
21. J. Classen, I. Rohr, C. Enss, S. Hunklinger, C. Laermans, Physica B **263-264**, 139 (1999).
22. S. Hunklinger, A.K. Raychaudhuri, in *Progress in Low Temperature Physics*, edited by D.F. Brewer (Elsevier, New York, 1986), Vol. 9, p. 265.
23. J. Classen, C. Enss, C. Bechinger, G. Weiss, S. Hunklinger, Ann. Phys. (Leipzig) **3**, 315 (1994).
24. J. Jäckle, Z. Phys. B **257**, 212 (1972).
25. X. Liu, B.E. White Jr., R.O. Pohl, Phys. Rev. Lett. **78**, 4418 (1997).
26. D. Tielbrger, R. Merz, R. Ehrenfels, S. Hunklinger, Phys. Rev. B **45**, 2750 (1992).
27. S. Rau, C. Enss, S. Hunklinger, P. Neu, A. Würger, Phys. Rev. B **52**, 7179 (1995).
28. P. Neu, A. Würger, Z. Phys. B **95**, 385 (1994).
29. P. Neu, A. Heuer, J. Chem. Phys. **106**, 1749 (1997).
30. V.G. Karpov, M.I. Klinger, F.N. Ignatev, Zh. Eksp. Teor. Fiz. **84**, 760 (1983) [Sov. Phys. JETP **57**, 439 (1983)]; Y.M. Galperin, V.G. Karpov, V.I. Kozub, Adv. Phys. **38**, 669 (1989); D.A. Parshin, Phys. Rev. B **49**, 9400 (1994).
31. P. Esquinazi, R. König, F. Pobell, Z. Phys. B **87**, 305 (1992).
32. A.J. Leggett, S. Chakravarty, A.T. Dorsey, M.P.A. Fisher, A. Garg, W. Zwerger, Rev. Mod. Phys. **59**, 1 (1987).
33. C.C. Yu, A.J. Leggett, Comments Cond. Mat. Phys. **14**, 231 (1988).
34. K. Kassner, R.J. Silbey, J. Phys. Cond. Matter **1**, 4599 (1989).
35. A.L. Burin, Yu. Kagan, Physica B **194–196**, 393 (1994).
36. A. Würger, Z. Phys. B **94**, 173 (1994); **98**, 561 (1995).
37. A. Würger, *Springer Tracts in Modern Physics* (Springer, New York, 1997), Vol. 135.
38. B.S. Berry, W.C. Pritchet, IBM J. Res. Develop. **19**, 334 (1975).
39. X. Liu, E. Thompson, B.E. White Jr., R.O. Pohl, Phys. Rev. B **59**, 11767 (1999).
40. R. Vacher, J. Pelous, Phys. Rev. B **14**, 823 (1976).
41. R. Vacher, J. Pelous, F. Plicque, A. Zarembowitch, J. Non-Cryst. Solids **45**, 397 (1981).
42. A.M. de Goër, M. Locatelli, C. Laermans, J. Phys. Colloq. France **42**, C6-78 (1981).
43. G. Weiss, A. Daum, M. Sohn, J. Arndt, Physica B **219&220**, 290 (1996).
44. Suprasil I is a SiO_2 glass containing about 1200 ppm hydroxyl ions. The elastic properties of this glass in its non-compacted state [43] are very similar to those of Suprasil W.
45. M.R. Vukcevich, J. Non-Cryst. Solids **11**, 25 (1972).
46. U. Buchenau, H.M. Zhou, N. Nücker, K.S. Gilroy, W.A. Phillips, Phys. Rev. Lett. **60**, 1318 (1988).
47. M.H. Cohen, G.S. Grest, Phys. Rev. Lett. **45**, 1271 (1980); Solid State Commun. **39**, 143 (1981).